

Zero-field splitting in pentacoordinate Co(II) complexes



C. Rajnák^{a,b}, J. Titiš^a, I. Šalitroš^{c,d}, R. Boča^{a,*}, O. Fuhr^d, M. Ruben^{b,d}

^a Department of Chemistry, FPV, University of SS Cyril and Methodius, SK-917 01 Trnava, Slovakia

^b Institute de Physique et Chimie de Matériaux de Strasbourg (IPCMS), UMR 7504 CNRS-Université de Strasbourg, F-67034 Strasbourg, France

^c Institute of Inorganic Chemistry, FCHPT, Slovak University of Technology, SK-812 37 Bratislava, Slovakia

^d Institute of Nanotechnology, Karlsruhe Institute of Technology, Hermann-von-Helmholtz-Platz 1, 76344 Eggenstein-Leopoldshafen, Germany

ARTICLE INFO

Article history:

Received 15 April 2013

Accepted 6 August 2013

Available online 14 August 2013

Keywords:

Cobalt(II) complex

Crystal structure

Zero-field splitting

Magnetostructural D-correlation

ABSTRACT

Pentacoordinate Co(II) complexes possessing the $\{\text{CoN}_3\text{X}_2\}$ chromophore ($\text{X} = \text{Cl}, \text{O}$) have been synthesized and structurally characterized. The magnetic data confirm high magnetic anisotropy expressed through the axial zero-field splitting parameter $D/hc = 50\text{--}70 \text{ cm}^{-1}$. These values lie between those found in tetraordinate and hexacoordinate Co(II) complexes.

© 2013 Elsevier Ltd. All rights reserved.

1. Introduction

Magnetostructural correlations are widely studied in literature since they form a basis for a relationship between structure and magnetoactivity of coordination compounds. Majority of attempts were focused to the correlation of the isotropic exchange coupling constant J versus an appropriate structural parameter – an M-X-M angle or M-X bond length within the superexchange path in binuclear or polynuclear complexes [1–15]. This type of correlation can be termed the magnetostructural J -correlations since recently another type has been outlined, namely the magnetostructural D -correlations. Here the axial zero-field splitting parameter D in mononuclear complexes is in a relation with the structural tetragonality.

In hexacoordinate Ni(II) complexes such a correlation is given by a straight line (in fact a pair of nearly collinear straight lines) and D -values vary between $D/hc = -8$ to $+8 \text{ cm}^{-1}$ [16–21]. In hexacoordinate Co(II) complexes, however, the correlation is represented by a set of parametric non-linear curves in the segment of the compressed tetragonal bipyramid [22–25]. In hexacoordinate Co(II) complexes the retrieved set of D -values spans the interval of $D/hc = +70$ to $+144 \text{ cm}^{-1}$ (always positive). In addition to magnetometry (temperature dependence of the magnetic susceptibility, and field dependence of the magnetization) also the FAR-IR spectra are helpful in a direct spectral determination of the D -parameter for centrosymmetric complexes [26–28]. In tetraordinate Co(II)

complexes a reliable data set started to be build up by combining the magnetometry, high-field/high-frequency EPR, and quantum-chemical calculations [29]. In tetraordinate complexes possessing the $\{\text{CoN}_2\text{X}_2\}$ and/or $\{\text{CoX}_4\}$ chromophores the D -values are much lower and could be either negative or positive: $D/hc = -15$ to $+40 \text{ cm}^{-1}$ [29–31]. Preliminary data show that D -values are more sensitive to the angular distortions of the reference tetrahedron; in addition to the T_d symmetry, D_{2d} , C_{2v} and C_1 frequently occur.

A logical step forward is to investigate the pentacoordinate Co(II) complexes. However, there are more structural parameters in the play, since in addition to the radial parameters in $\{\text{CoN}_3\text{X}_2\}$ chromophores also the angular coordinates vary: the angles $\alpha = \text{N-Co-N}$ and $\beta = \text{X-Co-X}$. The literature sources about of the magnetic parameters (D) in pentacoordinate Co(II) complexes are rather modest [32–35] so that the only way is to prepare a series of complexes and to investigate them by modern magnetometric hardware and magnetochemical software. A direct measurement of the energy gap by the high-frequency/high-field EPR technique meets difficulties since the estimated range of D -parameters (around 50 cm^{-1}) lies outside the capabilities of the existing hardware. Indirect EPR estimates, however, are at the disposal; they were based upon the spin lattice relaxation time as a basis for the determination of the lowest energy gap in a series of Co(II) complexes with coordination numbers 4, 5, and 6 [33].

A rational design of the zero-field parameter is a challenge of recent period. The D -parameter enters the formula for the barrier to spin reversal in single-molecule magnets ($\Delta = |D|S^2$) and therefore it is a first prerequisite of the magnetism at the molecular level [36]. The greater the D -parameter, the greater the barrier to spin

* Corresponding author. Tel.: +421 905763967.

E-mail address: roman.bocha@stuba.sk (R. Boča).

reversal Δ , and the longer the lifetime of the single-molecule magnets.

2. Experimental

2.1. General

Chemicals were purchased from Sigma–Aldrich and Merck and used as received. The solvents, *n*-hexane, Et₂O, EtOAc, CH₂Cl₂, CH₃OH were used without further purification; CH₃CN and (i-pr)₂NH were dried by distillation over CaH₂.

¹H and ¹³C NMR spectra were recorded using FT-NMR Spectrometer (Avance III 500 MHz, Bruker) with solvent proton as an internal standard. The infrared spectra in KBr pellets in the range 4000–400 cm⁻¹ were acquired at room temperature using FT-IR spectrometer (Spectrum GX, Perkin Elmer). Electron spectra were measured by UV–Vis–NIR spectrophotometer (Cary 500 Scan). Mass spectra were measured by microTOF-QII for ESI-TOF (Bruker). Elemental analyses were carried out on a Vario MICRO cube. For thin-layer chromatography silica plates POLYGRAM SIL G/UV₂₅₄ and alumina plates POLYGRAM ALOX N/UV₂₅₄ were used under the ultraviolet light at 254 nm. Melting points were determined Melting Point B-540 (Büchi).

The magnetic measurements were conducted using a SQUID apparatus (MPMS-XL7, Quantum Design) in the RSO mode of detection. About 20 mg of the sample was encapsulated in a gelatin-made sample holder. The susceptibility taken at *B* = 0.1 T has been corrected for the underlying diamagnetism and converted to the effective magnetic moment. The magnetization has been measured at two temperatures: *T* = 2.0 and *T* = 4.6 K.

2.2. Synthesis

The ligand 4'-iodo-2',6'-dipyrazolyl-pyridine (**L**¹) was synthesized following reported procedures [37–41].

The ligand 4'-dodecynyl-2',6'-dipyrazolyl pyridine (**L**²) was prepared as follows. In a 100 cm³ two necked round bottom flask, a freshly distilled (i-pr)₂NH (50 cm³) was deoxygenated under the Ar flux for 1 h. **L**¹ (0.674 g, 2 mmol), 10% of Pd⁰(PPh₃)₄ and CuI (0.038 g, 0.2 mmol) were suspended in an Ar-gas bubbled solution of (i-pr)₂NH and stirred for 1 h. 1-Dodecyne (0.665 g, 4 mmol) was added and the mixture was stirred for 3 days at RT. The solvent was removed using a rotary evaporator. The solid residue was at first column chromatographed on alumina with EtOAc/*n*-Hex (1:20, *R*_f = 0.50) as an eluent. The combined slightly yellowish solutions yielded upon evaporation and dried in vacuum to 0.35 g of a white powder (0.93 mmol, 46.6%). *Anal. Calc.* C₂₃H₂₉N₅: C, 73.57, H, 7.78; N, 18.65. Found: C, 73.59; H, 7.63; N, 18.59%. Melting point 53–55 °C. ¹H NMR [500 MHz, CDCl₃, 25 °C, δ/ppm]: 8.53 (d, 2H), 7.83 (s, 2H), 7.75 (t, 2H), 6.49 (dd, 2H), 2.45 (t, 2H), 1.61 (m, 2H), 1.44 (m, 2H), 1.29 (m, 12H), 0.87 (t, 3H). ¹³C NMR [125 MHz, CDCl₃, 25 °C, δ/ppm]: 150.10, 142.43, 137.73, 127.09, 111.69, 108.02, 97.46, 78.32, 31.92, 29.16, 22.70, 19.52, 14.13. UV–Vis (CH₂Cl₂): λ_{max} (ε, M⁻¹ cm⁻¹) = 251 (61204), 322 (16213). FT-IR (KBr): ν/cm⁻¹ = 3114, 3094, 2914, 2850, 2244, 1783, 1738, 1615, 1555, 1523, 1468, 1398, 1266, 1210, 1115, 1053, 1039, 959, 938, 856, 794, 757.

Single crystals for X-ray diffraction were grown from CH₃OH. Formula C₂₃H₂₉N₅; *M* = 375.51; *T* = 180(2) K; crystal system: monoclinic; crystal size/mm = 0.25 × 0.07 × 0.05; space group: *P*2(1)/*c*; *a* = 5.395(3) Å; *b* = 20.0348(10) Å; *c* = 19.9239(12) Å; α = 90°, β = 94.245(53)°, γ = 90°, *V* = 2147.6(2) Å³; *Z* = 4; ρ_{calc} = 1.161 g cm⁻³, μ(Mo Kα) = 0.71073 mm⁻¹; reflections measured: 4056, *F*(000) = 808, goodness-of-fit on *F*² = 0.881, final *R* indices

[*I* > 2σ(*I*): *R*₁ = 0.0482; *wR*₂ = 0.1005, *R* indices (all data): *R*₁ = 0.1041, *wR*₂ = 0.1163, extinction coefficient = 0.0193(17).

Preparation of the complex [CoCl₂L¹], **1**. In a 100 cm³ two necked round bottom flask a solution of **L**¹ (100 mg, 0.30 mmol) and CoCl₂·6H₂O (70.57 mg, 0.30 mmol) in CH₃CN (40 cm³) was heated at 80 °C for overnight under Ar flow. The reaction mixture was cooled down to room temperature. Blue block-shaped crystals were grown from diffusing the Et₂O into the CH₃CN solution of the complex under Ar at room temperature in several days. Yield 103.1 mg (0.22 mmol, 74.44%). *Anal. Calc.* C₁₁H₈Cl₂CoIN₅·0.45H₂O: C, 27.81; H, 1.89, N 14.74. Found: C, 27.75; H, 1.78; N, 14.74%. *θ*_f = 394–396 °C. ESI-TOF MS (CH₃CN): *m/z* = 430.86 [M]⁺. UV/VIS (Nujol): ν_{max}/10³ cm⁻¹ (absorbance) = 15.649 (0.247), 17.483 (0.201), 24.445 (0.600), 30.121 (1.078). FT-IR (KBr): ν/cm⁻¹ = 3340, 3207, 3108, 3096, 1602, 1561, 1519, 1496, 1453, 1414, 1390, 1335, 1271, 1216, 1205, 1173, 1136, 1078, 1050, 962, 923, 910, 861, 834, 788, 766, 745, 642, 601, 539.

Preparation of the complex [CoCl₂L²], **2**. In a 100 cm³ two necked round bottom flask a solution of **L**² (100 mg, 0.27 mmol) and CoCl₂·6H₂O (63.36 mg, 0.27 mmol) in CH₃CN (40 cm³) was heated at 80 °C for overnight under Ar flow. The reaction mixture was cooled down to room temperature. This compound was synthesized as described for **1**. Blue needle-shaped crystals were grown by evaporation of CH₃CN solution of the complex at the room temperature in several days. Yield 110 mg (0.218 mmol, 81.45 %). *Anal. Calc.* C₂₃H₂₉CoCl₂N₅·0.3H₂O: C, 54.09; H, 5.84 N, 13.71. Found: C, 53.99; H, 5.73; N, 13.67%. Melting point 276–278 °C. ESI-TOF MS (CH₃CN): *m/z* = 469.11 [M]. UV–Vis (Nujol): ν_{max}/10³ cm⁻¹ (absorbance) = 16.313 (0.172), 30.030 (0.977). FT-IR (KBr): ν/cm⁻¹ = 3107, 2922, 2852, 2218, 1618, 1553, 1525, 1495, 1453, 1402, 1399, 1266, 1225, 1171, 1049, 965, 901, 853, 791, 761, 629, 587, 480.

2.3. X-ray structure determination

Single crystal X-ray data were collected on a STOE IPDS II diffractometer with graphite monochromated Mo Kα radiation (λ = 0.71073 Å). Structure solution and refinement against *F*² were carried out using SHELXS and SHELXL software [42]. Refinement was performed with anisotropic temperature factors for all non-hydrogen

Table 1
Crystal data for compounds **1** and **2**.

	Complex 1	Complex 2
Empirical formula	C ₁₁ H ₈ Cl ₂ CoIN ₅	C ₂₇ H ₃₅ Cl ₂ CoN ₇
Formula weight (g mol ⁻¹)	466.95	587.45
Crystal system	monoclinic	orthorhombic
Space group	<i>P</i> 2(1)/ <i>c</i>	<i>P</i> bca
<i>T</i> (K)	180(2)	180(2)
Crystal size (mm)	0.21 × 0.12 × 0.11	0.24 × 0.09 × 0.01
<i>Z</i>	4	8
<i>a</i> (Å)	10.5357(8)	15.3677(5)
<i>b</i> (Å)	8.1978(7)	14.5418(6)
<i>c</i> (Å)	17.1482(11)	26.9215(10)
α (°)	90	90
β (°)	97.523(5)	90
γ (°)	90	90
<i>V</i> (Å ³)	1468.33(19)	6016.3(4)
Calculated density <i>D</i> _{calc} (g cm ⁻³)	2.112	1.297
Absorption coefficient (mm ⁻¹)	3.630	0.0776
Reflections collected/unique (<i>R</i> _{int})	5182/2421 [<i>R</i> (int) = 0.0422]	19388/5626 [<i>R</i> (int) = 0.0677]
Final <i>R</i> indices	<i>R</i> ₁ = 0.0304, <i>wR</i> ₂ = 0.0661	<i>R</i> ₁ = 0.0402, <i>wR</i> ₂ = 0.1065
<i>R</i> indices (all data)	<i>R</i> ₁ = 0.0465, <i>wR</i> ₂ = 0.0699	<i>R</i> ₁ = 0.0614, <i>wR</i> ₂ = 0.1226

atoms (disordered atoms were refined isotropically). The positions of the hydrogen atoms were calculated in idealized positions. The crystal data and the parameters of the structure refinement are listed in Table 1.

3. Results and discussion

3.1. Structure of complexes

The structure of the compound **1** is formed of molecular units ($Z = 4$) and no solvent molecules are present in the crystal lattice (Fig. 1). The coordination environment in the cobalt(II) metal ion refers to a distorted hexahedron. The Co–Cl bond lengths average to 2.269 Å, two Co–(imidazole) average to 2.188 Å, and the shortest one is Co–N(pyridine) = 2.071 Å (Table 2). According to the bond angles the polyhedron is derived from the trigonal bipyramid whose base is formed of the {N(pyridine)Cl₂} unit and the apical vertices are occupied by two N(imidazole) donor atoms. The N(imidazole)–Co–N(imidazole) angle amounts to 147.2 deg and is bisected by the N(pyridine) atom. The basal angle Cl–Co–Cl = 113.6 deg is lower relative to the ideal triangle.

The molecular structure of the complex **2** is very similar to **1** with analogous bond lengths and bond angles: averaged Co–Cl = 2.277 Å, Co–N(imidazole) = 2.151 Å, and Co–N(pyridine) = 2.061 Å. The critical bond angles are N(imidazole)–Co–N(imidazole) = 147.2° and Cl–Co–Cl = 112.2 deg. Two acetonitrile molecules co-crystallize per formula unit of **2** (see ESI, Fig. S4).

3.2. Magnetic properties

The complex **1** contains {CoN₃Cl₂} chromophore that keeps nearly the C_{2v} symmetry. One plane bisects the N–Co–N angle $\alpha = 147^\circ$ and the second one the Cl–Co–Cl angle $\beta = 114^\circ$. The chromophore was localized in the polar coordinate system with three N-atoms in the x – y plane and two Cl atoms pointing above and below that plane. Approximately the experimental geometry was adopted for calculations by the generalized crystal-field theory (GCFT) [43].

The GCFT method combines the electrostatic matrices (**A**), crystal-field potential at arbitrary position of ligands (**B**), spin–orbit interaction matrices (**C**), the matrices of the orbital (**D**) and spin angular momenta (**E**); the basis set covers all the components of the atomic terms of the given d^n electron configuration (120 components for d^7). The final assembly is diagonalized thus producing

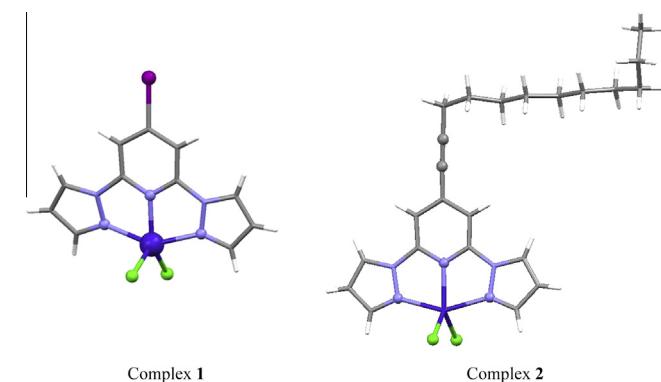


Fig. 1. Left – molecular structure of the compound **1** [CoCl₂L¹]. Bond distances within the chromophore at 180 K (in Å): Co1–N1(imidazole) = 2.175(4), Co1–N3(pyridine) = 2.071(4), Co1–N5(imidazole) = 2.202(4), Co1–Cl1 = 2.2729(14), Co1–Cl2 = 2.2654(14). Right – molecular structure of the complex **2** [CoCl₂L²]. Bond distances in the coordination polyhedron at 180 K (in Å): Co1–N1(imidazole) = 2.156(2), Co1–N3(pyridine) = 2.061(2), Co1–N5(imidazole) = 2.147(2), Co1–Cl1 = 2.2784(8), Co1–Cl2 = 2.2752(8). Hydrogen atoms are omitted for clarity.

Table 2

Bond lengths (Å) and bond angles (°) within chromophore of **1** and **2** at 180 K.

	1	2
Co1–N1(imidazole)	2.175(4)	2.156(2)
Co1–N3(pyridine)	2.071(4)	2.061(2)
Co1–N5(imidazole)	2.202(4)	2.147(2)
Co1–Cl1	2.2729(14)	2.2784(8)
Co1–Cl2	2.2654(14)	2.2752(8)
N(1)–Co(1)–Cl(1)	99.31(11)	96.58(7)
N(3)–Co(1)–Cl(1)	138.39(11)	125.88(7)
N(5)–Co(1)–Cl(1)	97.56(11)	99.34(7)
N(1)–Co(1)–Cl(2)	98.68(11)	98.58(7)
N(3)–Co(1)–Cl(2)	107.97(12)	121.94(7)
N(5)–Co(1)–Cl(2)	100.00(12)	98.10(7)
Cl(2)–Co(1)–Cl(1)	113.64(6)	112.17(3)

the eigenvalues: the crystal-field terms (**A** + **B**), crystal-field multiplets (**A** + **B** + **C**) and the Zeeman levels (**A** + **B** + **C** + **D** + **E**) for the reference magnetic field. The crystal-field poles were selected as follows: $F_4(N) = 8000 \text{ cm}^{-1}$ (intermediate field), and $F_4(Cl) = 6000 \text{ cm}^{-1}$ (weak field) simulating the tetragonal bipyramid. The only external parameters involved are the Racah parameters of the interelectron repulsion $B/hc = 989 \text{ cm}^{-1}$, $C/hc = 4253 \text{ cm}^{-1}$, and the spin–orbit coupling constant $\xi/hc = 515 \text{ cm}^{-1}$. As a result, the seven crystal-field terms arising from the free-atom ⁴F-term lie at energies 0, 1870, 2380, 3930, 4400, 9570, and 9950 cm^{-1} (the labels ⁴A or ⁴B are a matter of the coordinate system).

Having the eigenvalues and eigenvectors for the crystal-field terms at the disposal, the calculation proceeds in evaluating the Cartesian components of the spin–spin interaction tensor D_{ab} by means of the perturbation theory. Its individual components, of course, depend upon the choice of the coordinate system; the tensor as a whole stays invariant. Therefore the system under study can be placed arbitrarily in the coordinate system and the conventional relationship between magnetic parameters D and E ($|D| > 3E$) can be fixed afterwards by simple rotations.

Owing to the close-lying excited terms, rather high values of the zero-field splitting parameters were calculated by GCFT: $D/hc = -42$ and $E/hc = 19 \text{ cm}^{-1}$. Their sign is a matter of the reference coordinate system since for the Kramers system only the energy gap $\Delta = 2(D^2 + 3E^2)^{1/2}$ is invariant giving rise to $\Delta/hc = 107 \text{ cm}^{-1}$. Notice, the D-tensor components were $D_{xx} = 0$, $D_{yy} = -38.5$, $D_{zz} = -60.8$ [in cm^{-1}] which after a rearrangement $x \rightarrow z \rightarrow y \rightarrow x$ yield $D = D_{zz} - (D_{xx} + D_{yy})/2 = 49.6$ and $E = (D_{xx} - D_{yy})/2 = 11.1 \text{ cm}^{-1}$; again $\Delta/hc = 107 \text{ cm}^{-1}$. The last choice of coordinates satisfies $|D| > 3E$. At the same time, $g_x = 2.000$, $g_y = 2.451$, $g_z = 2.711$ ($g_{av} = 2.39$) was calculated by GCFT which after the above rearrangement yields $g_x = 2.451$, $g_y = 2.711$, $g_z = 2.000$. The energy gap between the ground ($\Gamma_5 + \Gamma_6$) and the first excited (Γ_4) crystal-field multiplets was calculated beyond the spin-Hamiltonian formalism when the spin–orbit interaction is explicitly included into the interaction matrix. Then the energy gap reads $\Delta_m/hc = 99 \text{ cm}^{-1}$.

The above analysis is helpful in getting a trial set of magnetic parameters for fitting the susceptibility and magnetization data. The effective magnetic moment for **1** adopts a value of $\mu_{\text{eff}} = 4.7 \mu_B$. at the room temperature and on cooling is slightly decreases until ca 100 K when its drop is more rapid: at $T = 2.0 \text{ K}$ it adopts a value of $\mu_{\text{eff}} = 3.4 \mu_B$ (Fig. 2). Based upon a formula $\mu_{\text{eff}}/\mu_B = g_{av} [S(S+1)]^{1/2}$, the high-temperature limit allows an estimate of $g_{av} = 2.4$. The magnetization per formula unit at $T = 2.0 \text{ K}$ and $B = 7 \text{ T}$ saturates to the value of $M_1 = M_{\text{mol}}/N_A \mu_B = 2.3$ that confirms a sizable zero-field splitting.

The fitting procedure has been based upon minimization of a functional $F = R(\chi) \times R(M)$ that combines relative errors in susceptibility and magnetization. The conventional spin Hamiltonian

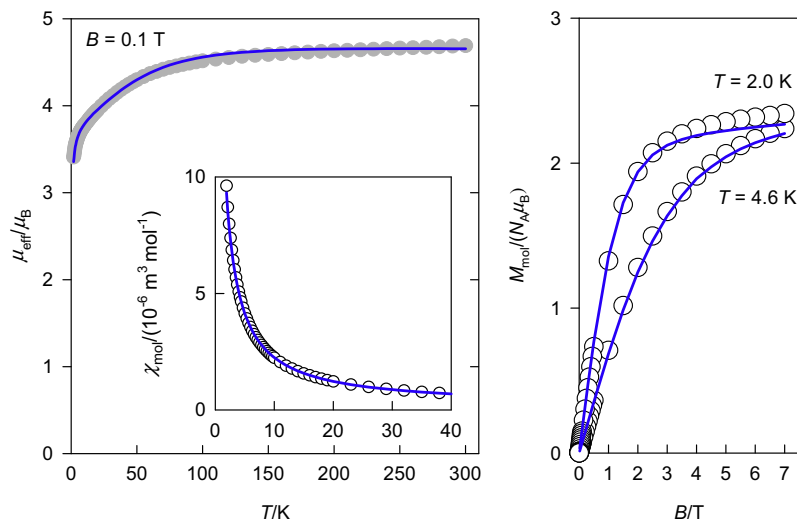


Fig. 2. Magnetic data for **1**: left – temperature dependence of the effective magnetic moment; right – field dependence of the magnetization. Circles – experimental data, solid lines – fitted.

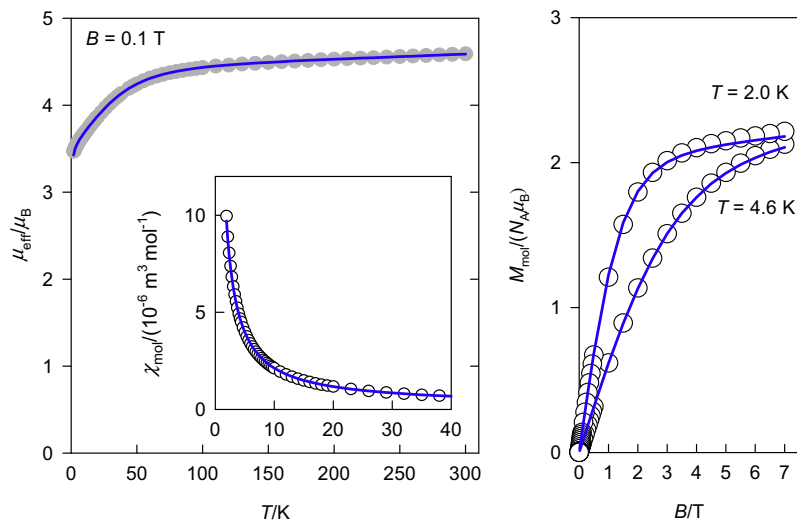


Fig. 3. Magnetic data for **2**: left – temperature dependence of the effective magnetic moment; right – field dependence of the magnetization. Circles – experimental data, solid lines – fitted.

$$\hat{H}_{k,l} = D(\hat{S}_z^2 - \bar{S}^2/3)h^{-2} + E(\hat{S}_x^2 - \hat{S}_y^2)h^{-2} + \mu_B B_m (g_x \sin \nu_k \cos \phi_l \hat{S}_x + g_y \sin \nu_k \sin \phi_l \hat{S}_y + g_z \cos \nu_k \hat{S}_z)h^{-1} \quad (1)$$

has been used in generating the magnetic energy levels from which the susceptibility and magnetization were reconstructed by means of the apparatus of statistical thermodynamics [44]. The powder average has been provided by the Zeeman term distributed uniformly over 120 points (k, l) at one hemisphere. To this end the following set of magnetic parameters was received: $D/hc = +71.7 \text{ cm}^{-1}$, $E = 0.0$, $g_z = 2.00$, $g_y = g_x = 2.51$, $\chi_{\text{TIM}} = +0.1 \times 10^{-9} \text{ m}^3 \text{ mol}^{-1}$, $(zj)/hc = -0.075 \text{ cm}^{-1}$; $R(\chi) = 0.015$, $R(M) = 0.021$. This solution is displayed in Fig. 2 (solid lines). With this set of parameters the energy gap is $\Delta = 2D = 143 \text{ cm}^{-1}$.

The complex **2** belongs to the same family as the complex **1** so that the same model has been applied for the magnetic data analysis (Fig. 3). The fitting procedure gave $D/hc = +46.8 \text{ cm}^{-1}$, $E = 0.0$, $g_z = 2.00$, $g_y = g_x = 2.35$, $\chi_{\text{TIM}} = +9.0 \times 10^{-9} \text{ m}^3 \text{ mol}^{-1}$, $(zj)/hc = -0.026 \text{ cm}^{-1}$; $R(\chi) = 0.012$, $R(M) = 0.0094$.

The preparation and magnetic properties of the complex [Co(*bzimpy*)Cl₂] **3** with the tridentate ligand *bzimpy* = 2,6-bis(benzimidazol-2'-yl)pyridine, containing the {CoN₃Cl₂} chromophore, have been reported elsewhere [45]. The magnetic data were fitted with $D/hc = 73.4$, $E/hc = 3.3 \text{ cm}^{-1}$, $g_z = 1.51$, $g_x = 2.50$, $g_y = 2.62$, $zj/hc = -0.250 \text{ cm}^{-1}$, $\chi_{\text{TIM}} = 2.22 \times 10^{-9} \text{ m}^3 \text{ mol}^{-1}$. The magnetic data have been remeasured at the same conditions as previous complexes (Fig. 4). The revised magnetic parameters are: $D/hc = +61.9 \text{ cm}^{-1}$, $E = 0.0$, $g_z = 2.00$, $g_y = g_x = 2.34$, $\chi_{\text{TIM}} = +2.86 \times 10^{-9} \text{ m}^3 \text{ mol}^{-1}$, $(zj)/hc = 0 \text{ cm}^{-1}$; $R(\chi) = 0.015$, $R(M) = 0.057$.

The complex [Co(*saldptm*)] **4** with *saldptm* = N,N'-bis(3-^tbutyl-2-hydroxy-5-benzyliden)-1,7-diamino-4-methyl-4-azaheptane contains the {CoN₃O₂} chromophore that resembles some similarities with **1** and **2** (Fig. 5). Its preparation and magnetic studies already have been reported elsewhere; the SQUID magnetic data were fitted with the following set of magnetic parameters: $D/hc = 48.4 \text{ cm}^{-1}$, $E/hc = 0$, $g_x = g_y = 2.62$, $g_z = 2.06$, $\chi_{\text{TIP}} = 3.7 \times 10^{-9} \text{ m}^3 \text{ mol}^{-1}$ [46,47]. A reinvestigation gave: $D/hc = +52.0 \text{ cm}^{-1}$, $E/hc = 0$, $g_x = g_y = 2.60$, $g_z = 2.0$, $\chi_{\text{TIP}} = 20 \times 10^{-9} \text{ m}^3 \text{ mol}^{-1}$; $R(\chi) = 0.023$, $R(M) = 0.044$.

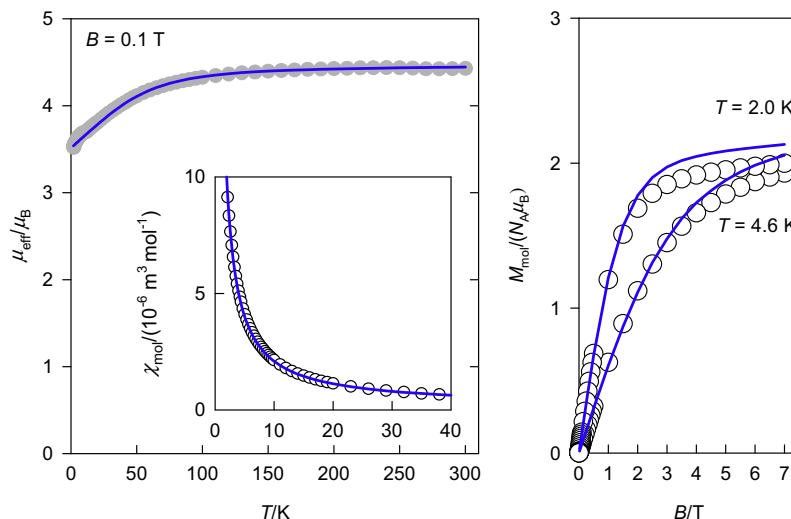


Fig. 4. Magnetic data for [Co(bzimpy)Cl₂] **3**: left – temperature dependence of the effective magnetic moment; right – field dependence of the magnetization. Circles – experimental data, solid lines – fitted.

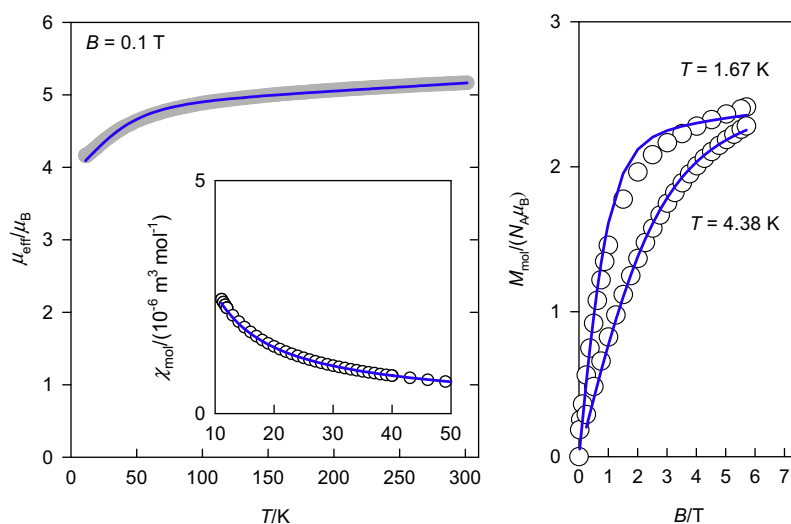


Fig. 5. Magnetic data for [Co(saldptm)] **4**: left – temperature dependence of the effective magnetic moment; right – field dependence of the magnetization. Circles – experimental data, solid lines – fitted.

3.3. Wide-range modeling

In order to determine limits for the zero-field splitting in penta-coordinate Co(II) complexes a wide-range modeling has been done by means of the generalized crystal-field theory. The initial geometry has been chosen in D_{3h} symmetry referring to the trigonal bipyramid for the $\{CoX_2B_2\}$ chromophore with the polar coordinates (θ, ϕ) being X(90, 0), A(0, 180) and A'(180, 180), B(90, 90) and B'(90, -90) deg. Then the angles $\theta(A)$ and $\phi(B)$ have been varied stepwise until A(30, 180) and B(90, 120) deg when the system again adopts the D_{3h} symmetry. The mapping of the total energy of the ground crystal-field term is shown in Fig. 6 – left; the tetragonal pyramid of the C_{4v} symmetry has energy much higher. The calculated crystal-field terms have been used in evaluating the zero-field splitting parameters D and E by means of the perturbation theory for non-degenerate states. Their actual values and signs depend upon the actual geometry but the energy gap $\Delta = 2(D^2 + 3E^2)^{1/2}$ stays invariant. However, at (near) degeneracy

the perturbation theory diverges and then D , E , and Δ parameters adopt incorrect values (Fig. 6 – centre). When the spin-orbit coupling is involved *via* variation method, the exact multiplet splitting $\Delta\Gamma$ is calculated; these values are well valid also for the degenerate crystal-field terms. This modeling (Fig. 6 – right) shows the limits of the energy gap which for the applied weak crystal-field ($F_4 = 6000\text{ cm}^{-1}$) ranges between $\Delta\Gamma = 73\text{ cm}^{-1}$ (D_{3h}) to 219 cm^{-1} (C_{4v}). For a stronger crystal field ($F_4 = 8000\text{ cm}^{-1}$) the situation is analogous with the limiting values shifted to $\Delta\Gamma = 57\text{ cm}^{-1}$ (D_{3h}) and 218 cm^{-1} (C_{4v}).

To this end: the zero-field splitting D -values (or better the energy gap Δ) are well described by the perturbation theory for the geometries close to the trigonal bipyramid when the ground crystal-field term is non-degenerate. On the contrary, the spin Hamiltonian formalism fails near the geometry of the tetragonal pyramid because of the degenerate ground term: in Fig. 6 (centre) the cutoff 200 cm^{-1} is applied. In such a case the modeling (or magnetic data fitting) need be performed beyond the spin-Hamil-

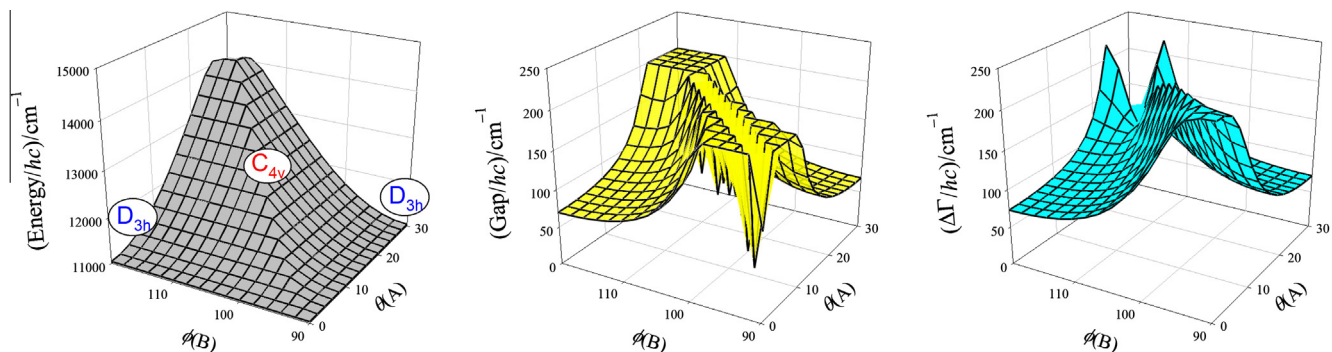


Fig. 6. Mapping of the total energy (left), zero-field energy gap Δ (center, cutoff 200 cm^{-1}), and the multiplet splitting (right) for the pentacoordinate Co(II) complexes; all crystal-field poles $F_4 = 6000\text{ cm}^{-1}$.

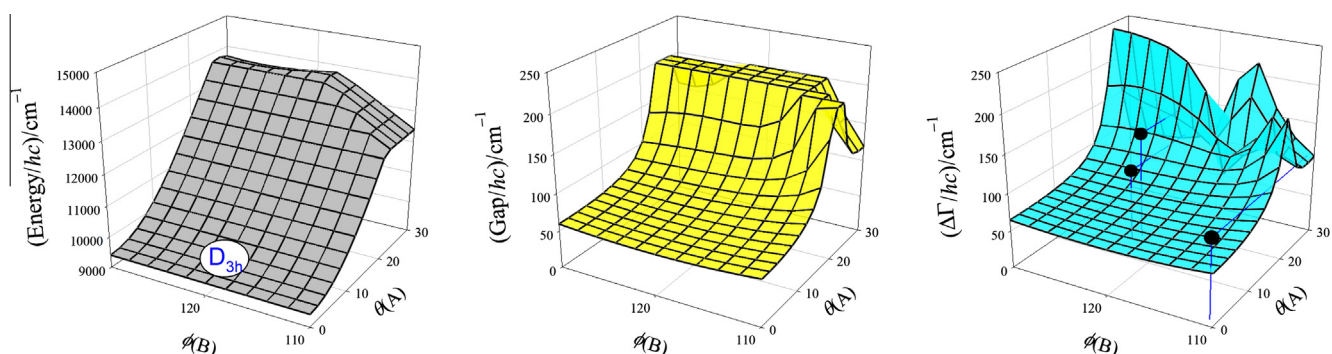


Fig. 7. Mapping of the total energy (left), zero-field energy gap Δ (center, cutoff 200 cm^{-1}), and the multiplet splitting (right) for the pentacoordinate Co(II) complexes; crystal-field poles $F_4(A) = 8000\text{ cm}^{-1}$, $F_4(B) = 6000\text{ cm}^{-1}$.

Table 3

Geometric and magnetic data for the pentacoordinate Co(II) complexes.

Complex ^a	Chromophore {CoXA ₂ B ₂ }	Angle A–Co–A (°)	Angle B–Co–B (°) (α)	$\theta(A)$ (°)	$\phi(B)$ (°)	β (°)	τ (°) ^b	$2D_{SH}$ (cm ⁻¹)	Technique Ref.
1	{CoNN ₂ Cl ₂ }	147.2	113.6	16.4	123.2	212.8	(1.65)	143	this work
2	{CoNN ₂ Cl ₂ }	150.6	112.2	14.7	123.6	209.4	(1.62)	98	this work
4	{CoNN ₂ O ₂ }	177.1	138.6	1.5	110.7	182.9	0.74	104	this work
{Co(<i>pno</i>) ₃ }(ClO ₄) ₂	{CoOO ₂ O ₂ }	173.4	129.8	3.3	115.1	173.4	0.73	(25)	EPR [33]
Co(<i>mpao</i>) ₄ (ClO ₄) ₂	{CoOO ₂ O ₂ }	n.a.					–	(18.9)	EPR [33]
{Co(Et ₄ <i>dien</i>)Cl ₂ }	{CoNNCINCl} ^c [48]	173.4	105.9			173.4	1.12	98	MCD [34]
{Co(Me ₆ <i>tren</i>)Cl}Cl	{CoClN ₂ N ₂ } [49] ^d	180.0	117.6			180	1.04	5.4	MCD [34]
								10	Suscept. [35]
{Co(Me ₆ <i>tren</i>)NCS}NCS	{CoNN ₂ N ₂ } [50] ^e	178.8	111.5			178.8	1.12	2.7	MCD [34]

^a Abbreviations: *pno* – 2-picoline-*N*-oxide, *mpao* – methyldiphenylarsanoxide.

^b $\tau = (\beta - \alpha)/60$; $\tau = 1$ for an ideal trigonal bipyramid and $\tau = 0$ for an ideal square pyramid.

^c Very distorted structure.

^d Bromo-analogue Co(Me₆*tren*)Br₂.

^e Nickel analogue [Ni(Me₆*tren*)NCS]NCS·H₂O.

tonian formalism when the spin–orbit coupling is involved via the variation method.

The modeling has been done also for the geometries close to **1** and **2** when the angle A–Co–A < 180°; the results are displayed in Fig. 7. It can be seen that for the geometries close to the trigonal bipyramid the energy gap Δ predicted by the spin-Hamiltonian formalism is close to the exact multiplet splitting $\Delta\Gamma$ calculated via the variation method. The last graph involves also three points according to Table 3 for which geometric and spin-Hamiltonian data are available. The drop-lines indicate a deviation from the prediction surface.

4. Conclusions

Pentacoordinate Co(II) complexes show a rather large magnetic anisotropy measured by the axial zero-field splitting parameter $D/hc = 50$ to 70 cm^{-1} . This interval lies in between tetracoordinate and hexacoordinate Co(II) complexes. The spin-Hamiltonian formalism is legitimate to apply in the vicinity of the trigonal bipyramid (D_{3h} symmetry) when the ground crystal-field term is non-degenerate. Near the geometry of the tetragonal bipyramid (C_{4v} symmetry) the ground term is (quasi) degenerate and consequently the spin-Hamiltonian formalism diverges. In such a case

the modeling and/or magnetic data fitting need be performed beyond the spin/Hamiltonian formalism.

Acknowledgements

Grant Agencies (Slovakia: VEGA 1/0233/12, APVV-0014-11) are acknowledged for the financial support.

Appendix A. Supplementary data

CCDC 932519 and 932520 contains the supplementary crystallographic data for **1** and **2**. These data can be obtained free of charge via <http://www.ccdc.cam.ac.uk/conts/retrieving.html>, or from the Cambridge Crystallographic Data Centre, 12 Union Road, Cambridge CB2 1EZ, UK; fax: (+44) 1223 336 033; or e-mail: deposit@ccdc.cam.ac.uk. Supplementary data associated with this article can be found, in the online version, at <http://dx.doi.org/10.1016/j.poly.2013.08.029>.

References

- [1] S. Youngme, J. Phatchimkun, N. Wannarit, N. Chaichit, S. Meejoo, G.A. van Albada, J. Reedijk, *Polyhedron* 27 (2008) 304.
- [2] G. Christou, S.P. Perlepes, E. Libby, K. Folting, J.C. Huffman, R.J. Webb, D.N. Hendrickson, *Inorg. Chem.* 29 (1990) 3657.
- [3] S.P. Perlepes, J.C. Huffman, G. Christou, *Polyhedron* 10 (1991) 2301.
- [4] S.P. Perlepes, J.C. Huffman, G. Christou, S. Paschalidou, *Polyhedron* 14 (1995) 1073.
- [5] T. Tokii, M. Nagamatsu, H. Hamada, M. Nakashima, *Chem. Lett.* (1992) 1091.
- [6] W. Huang, D. Hu, S. Gou, H. Qian, H.-K. Fun, S.S.S. Raj, Q. Meng, *J. Mol. Struct.* 649 (2003) 269.
- [7] B. Graham, M.T.W. Hearn, P.C. Junk, C.M. Kepert, F.E. Mabbs, B. Moubaraki, K.S. Murray, L. Spiccia, *Inorg. Chem.* 40 (2001) 1536.
- [8] T.M. Rajendiran, R. Kannappan, R. Venkatesan, P.S. Rao, M. Kandaswamy, *Polyhedron* 18 (1999) 3085.
- [9] I. Chadjistamatis, A. Terzis, C.P. Raptoulou, S.P. Perlepes, *Inorg. Chem. Commun.* 6 (2003) 1365.
- [10] M. Lubben, R. Hage, A. Meetsma, K. Byma, B.L. Feringa, *Inorg. Chem.* 34 (1995) 2217.
- [11] S. Youngme, C. Chailuecha, G.A. van Albada, C. Pakawatchai, N. Chaichit, J. Reedijk, *Inorg. Chim. Acta* 357 (2004) 2532.
- [12] S. Youngme, C. Chailuecha, G.A. van Albada, C. Pakawatchai, N. Chaichit, J. Reedijk, *Inorg. Chim. Acta* 358 (2005) 1068.
- [13] C. Chailuecha, S. Youngme, C. Pakawatchai, N. Chaichit, G.A. van Albada, J. Reedijk, *Inorg. Chim. Acta* 359 (2006) 4168.
- [14] S.M. Gorun, S.J. Lippard, *Inorg. Chem.* 30 (1991) 1625.
- [15] N.A. Law, J.W. Kampf, V.L. Pecoraro, *Inorg. Chim. Acta* 297 (2000) 252.
- [16] P. Baran, M. Boča, R. Boča, A. Krutošiková, J. Miklovič, J. Pelikán, J. Titiš, *Polyhedron* 24 (2005) 1510.
- [17] A. Mašlejová, R. Ivaníková, I. Svoboda, B. Papánková, L. Dlháň, D. Mikloš, H. Fuess, R. Boča, *Polyhedron* 25 (2006) 1823.
- [18] R. Ivaníková, R. Boča, L. Dlháň, H. Fuess, A. Mašlejová, V. Mrázová, I. Svoboda, J. Titiš, *Polyhedron* 25 (2006) 3261.
- [19] J. Titiš, R. Boča, Ľ. Dlháň, T. Ďurčėková, H. Fuess, R. Ivaníková, V. Mrázová, B. Papánková, I. Svoboda, *Polyhedron* 26 (2007) 1523.
- [20] R. Boča, J. Titiš, In *Coordination Chemistry Research Progress*, Nova Science Publishers, New York, 2008, p. 247.
- [21] J. Titiš, R. Boča, *Inorg. Chem.* 49 (2010) 3971.
- [22] A. Packová, J. Miklovič, J. Titiš, M. Koman, R. Boča, *Inorg. Chem. Commun.* 32 (2013) 9.
- [23] C. Rajnák, *Monatsh. Chem.* 142 (2011) 789.
- [24] J. Titiš, J. Hudák, J. Kožíšek, A. Krutošiková, J. Moncol, D. Tarabová, R. Boča, *Inorg. Chim. Acta* 388 (2012) 106.
- [25] J. Titiš, R. Boča, *Inorg. Chem.* 50 (2011) 11838.
- [26] B. Papánková, R. Boča, Ľ. Dlháň, I. Nemeč, J. Titiš, I. Svoboda, H. Fuess, *Inorg. Chim. Acta* 363 (2010) 147.
- [27] M. Šebová, R. Boča, Ľ. Dlháň, I. Nemeč, B. Papánková, J. Pavlik, H. Fuess, *Inorg. Chim. Acta* 383 (2012) 143.
- [28] M. Idešicová, R. Boča, *Inorg. Chim. Acta* (submitted).
- [29] M. Idešicová, J. Titiš, R. Boča, J. Krzystek, *Inorg. Chem.* 52 (2013) 9409.
- [30] M. Idešicová, Ľ. Dlháň, J. Moncol, J. Titiš, R. Boča, *Polyhedron* 36 (2012) 79.
- [31] J. Titiš, J. Miklovič, R. Boča, *Inorg. Chem. Commun.* 35 (2013) 72.
- [32] R. Boča, *Coord. Chem. Rev.* 248 (2004) 757.
- [33] M.V. Mäkinen, L.C. Kuo, M.B. Yim, G.B. Wells, J.M. Fukuyama, J.E. Kim, *J. Am. Chem. Soc.* 107 (1985) 5245.
- [34] J.A. Larrabee, C.M. Alessi, E.T. Asiedu, J.O. Cook, K.R. Hoerning, L.J. Klingler, G.S. Okin, S.G. Santee, T.L. Volkert, *J. Am. Chem. Soc.* 119 (1997) 4182.
- [35] D.M. Duggan, D.N. Hendrickson, *Inorg. Chem.* 14 (1975) 1944.
- [36] D. Gatteschi, R. Sessoli, J. Villain, *Molecular Nanomagnets*, Oxford University Press, Villain, 2006.
- [37] C. Rajadurai, Z. Qu, Z. Fuhr, Z. Gopalan, R. Kruk, M. Ghafari, M. Ruben, *Dalton Trans.* (2007) 3531.
- [38] C. Rajadurai, F. Schramm, O. Fuhr, M. Ruben, *Eur. J. Inorg. Chem.* (2008) 2649.
- [39] C. Rajadurai, O. Fuhr, R. Kruk, M. Ghafari, M. Hahn, M. Ruben, *Chem. Commun.* (2007) 2636.
- [40] N.T. Madhu, I. Šalitraš, F. Schramm, S. Klyatskaya, O. Fuhr, M. Ruben, C. R. Chim. 11 (2008) 1166.
- [41] I. Šalitraš, J. Pavlik, R. Boča, O. Fuhr, Ch. Rajadurai, M. Ruben, *Cryst. Eng. Commun.* 12 (2010) 2361.
- [42] G.M. Sheldrick, *Acta Crystallogr., Sect. A* 64 (2008) 112.
- [43] R. Boča, *Struct. Bonding* 117 (1996) 1.
- [44] R. Boča, *A Handbook of Magnetochemical Formulae*, Elsevier, Amsterdam, 2012.
- [45] R. Boča, Ľ. Dlháň, W. Linert, H. Ehrenberg, H. Fuess, W. Haase, *Chem. Phys. Lett.* 307 (1999) 359.
- [46] R. Boča, H. Elias, W. Haase, M. Huber, R. Klement, L. Muller, H. Paulus, I. Svoboda, M. Valko, *Inorg. Chim. Acta* 278 (1998) 127.
- [47] R. Herchel, R. Boča, *Dalton Trans.* (2005) 1352.
- [48] Z. Dori, R. Eisenberg, H.B. Gray, *Inorg. Chem.* 6 (1967) 483.
- [49] M. DiVaira, P.L. Orioli, *Inorg. Chem.* 6 (1967) 955.
- [50] I. Bertini, M. Ciampolini, D. Gatteschi, *Inorg. Chem.* 12 (1973) 2254.